Low-cost Wearable Device based D-shaped single mode fiber curvature sensor for Vital Signs Monitoring

Jie Li,[1] Bin Liu,[1,*] Juan Liu,[1] Jiu-Lin Shi, Xing-Dao He,[1] Jinhui Yuan[3, *] and Qiang Wu[1,2, *]

[1]*Key Laboratory of Opto-Electronic Information Science and Technology of Jiangxi Province, Nanchang Hangkong University, Nanchang 330063, China*

[2]*Faculty of Engineering and Environment, Northumbria University, Newcastle Upon Tyne, NE1 8ST, United Kingdom*

[3]*Research Center for Convergence Networks and Ubiquitous Services, University of Science & Technology Beijing, Beijing 100083, China*

** Corresponding authors: liubin_d@126.com; qiang.wu@northumbria.ac.uk; yuanjinhui81@163.com*

Abstract:

A low-cost wearable pulse and respiratory monitoring system based on D-shaped single mode fiber (SMF) curvature sensor is proposed and investigated. The curvature sensing performance of D-shaped SMFs with different transmission loss are tested and analyzed, and the sensitivity up to -7.208 %/m^{-1}. The D-shaped optical fiber structure is encapsulated by polydimethylsiloxane (PDMS) and implanted in a wrist strap, which realizes good wearability and comfort in the process of human pulse monitoring. The system adopts laser source module and signal acquisition module for integrated and miniaturized design, and real time signal acquisition using Field-Programmable Gate Array (FPGA). The real-time monitoring of pulse signal intensity and frequency before and after exercise was realized. The results show that pulse intensity increased after exercise, with a 10 %-30 % increase in pulse frequency, which is consistent with the results in medical theory. In addition, the D-shaped SMF encapsulated by PDMS also was implanted into the belt, which also successfully applied to the monitoring of respiratory signals under quiet and walking conditions.

Keywords: curvature sensor, D-shaped fiber, wearable device, pulse, respiration

1. Introduction

Pulse signal and respiratory signal are important health parameters in human physiological activities. Pulse frequency can be used to diagnose diseases such as increased intracranial pressure, atrioventricular block and digitalis poisoning. Respiratory rate can be used to diagnose fever, anemia, hyperthyroidism, heart failure and other diseases [1-7]. Traditional pulse sensors include flexible pulse sensors [8], radio frequency identification (RFID) ring pulse sensors [9], millimeter-wave pulse sensors [10], electronic pulse sensors [11], etc. However, these pulse sensors have more or less some problems in the process of use. For example, electronic pulse sensors are easily interfered by external factors such as electromagnetic waves in the process of monitoring. Traditional respiration monitoring methods include pressure sensing [12] and temperature sensing [13]. Pressure sensors are very sensitive, but the monitoring results are easily affected by various factors. Temperature sensors tend to make patients uncomfortable because the sensors are in contact with human skin directly. Traditional health monitoring equipment is expensive, bulky and inconvenient to use.

In order to realize high precision real-time monitoring of human health parameters, monitoring equipment based on optical fiber sensor has attracted the attention of relevant researchers [14-17]. The advantages of optical fiber sensors are outstanding, including high sensitivity, small size and strong anti-electromagnetic interference ability [18]. Some optical fiber sensors have been applied to human health monitoring, including fiber bragg grating (FBG) [19-22], optical fiber Michelson interferometer [23], Fabry-Perot (FP) interferometer [24-25], Mach–Zehnder interferometer (MZI) [26-27], Sagnac interferometer [28] and intensity modulation fiber [29-31], etc. In 2018, Y. Xiao *et al*, proposed an MZI based optical fiber sensor to achieve simultaneous measurement of urine sugar and microvelocity [32]. In 2019, A. Aitkulov *et al*, proposed an integrated sensing system combining POF sensors with smart phones to extract respiratory cycle information in time domain and frequency domain [33]. In 2020, Y. Li, *et al* proposed breathing process monitoring with a biaxially oriented polypropylene (BOPP) film based fiber FP sensor [34], and in 2021, M. Życzkowski *et al*, proposed the application of Sagnac Interferometer in monitoring human heart activity [35]. In 2021, N. V. Kumar *et al* proposed blood pressure pulse monitor based on fiber grating sensor [36]. In 2021, Y. L. Wang *et al*. proposed a low-cost wearable respiratory monitoring system based on D-shaped plastic fiber, which can monitor the respiratory frequency of human body in real time [37]. However, the above health monitoring system has some disadvantage, either high cost of equipment, or complex structure, low sensitivity, difficult to operate, such as the manufacturing cost of FBG is higher than that of SMF, and the demodulation of FBG is far more complex than that of SMF.

In this paper, a D-shaped optical fiber curvature sensor is proposed, and its curvature sensing characteristics are optimized and tested. The laser diode and its driving circuit, photodiode and its amplifying circuit are integrated and miniaturized in the system, which realized the low-cost design of the system. The sensor structure is encapsulated in PDMS and implanted in wrist strap or belt with good wearable, reliable and comfort, to realize the real-time monitoring of pulse and respiratory signals.

2. Curvature sensing principle and performance

When the single-mode fiber is bent and the bending radius is larger than the critical bending radius, the transmission loss caused by bending is very small, and the single-mode fiber is insensitive to bending. In order to improve the sensitivity of curvature sensing of single-mode fiber and realize highly sensitive monitoring of external signals, polishing the single-mode fiber is proposed in this paper [38-40]. After side polishing, the optical fiber is D-shaped. The light transmitted inside the optical fiber is in direct contact with the external environment. When the side polished region of the optical fiber is deformed, there is no cladding in this region, and the optical signal loss occurs greatly. The sensitivity of the fiber to the external environment and the linearity of the signal attenuation of the sensor are greatly improved when the single-mode fiber is polished [41-43].

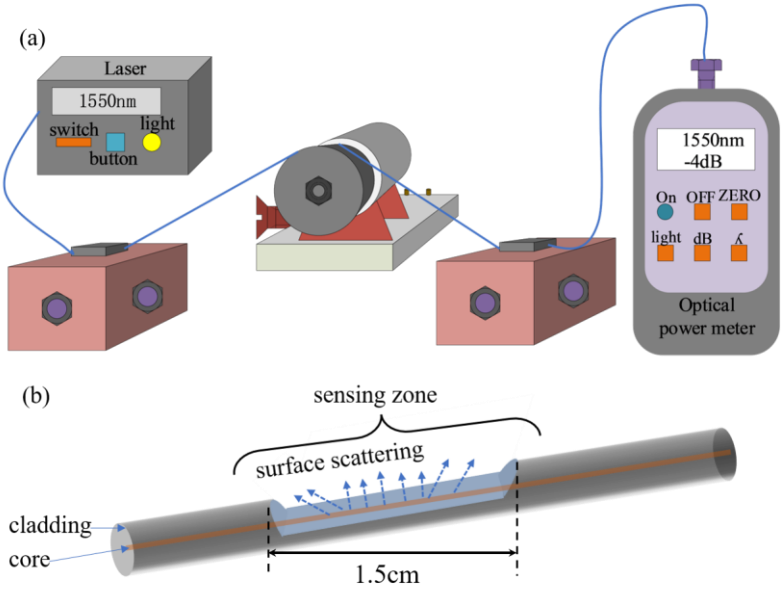

Fig. 1. (a) Polished system; (b) Optical fibers after polishing.

The set of fiber side-polished system have been built to process and prepare D-shaped fiber, which is shown in Fig. 1(a). One end of the SMF is connected to a laser light source with a wavelength of 1550 nm, and the other end is connected to an optical power meter, which is used to monitor the side polish depth of the optical fiber in real time. The side polishing wheel is driven and controlled by the DC power supply to polish the single-mode fiber. The roughness of the sandpaper on the surface of the wheel is 3000 mesh, which ensures that the optical fiber will not break during polishing and the surface of the optical fiber after

side polishing is relatively smooth. Finally, D-shaped optical fiber curvature sensor is fabricated, and the length of polished SMF is 1.5 cm, which is determined by the distance between the translation stages at both ends, as shown in Fig. 1(b). In the process of side polish, when the side polish depth is close to the single-mode fiber core [shown in Fig. 1(b)], the transmission power will attenuate significantly, and the deeper the side polish depth at the fiber core, the greater the transmission loss. Five D-shaped optical fibers with different side polish depths were fabricated, and the transmission loss of D-shaped optical fibers varied as -2 dB, -4 dB, -6 dB, -8 dB and -10 dB, respectively. The curvature sensing characteristics of D-shaped optical fibers were tested and analyzed. As shown in Fig. 2, the side-polishing optical fiber is fixed at both ends of the translation stage with the side-polishing surface up. The initial distance between A and B is fixed at 2.5 cm, denoted as L_{AB}. Both ends of the optical fiber are connected with a 1550 nm laser source and an optical power meter to measure the optical power of the side-polished optical fiber. Rotate the displacement knob of the optical translation stage, and move 5 μm (denoted as Δy) each time for 9 times. After each move, record the indicator of the optical power meter. The calculation formula of curvature [44]:

$$C=2\frac{\sin(\frac{L_{AB}C}{2})}{L_{AB}-\Delta y}\approx\sqrt{\frac{24\Delta y}{L_{AB}^3}} \tag{1}$$

where C is the curvature of optical fiber, L_{AB} is the initial distance between A and B, Δy is the distance of each movement of the optical translation stage.

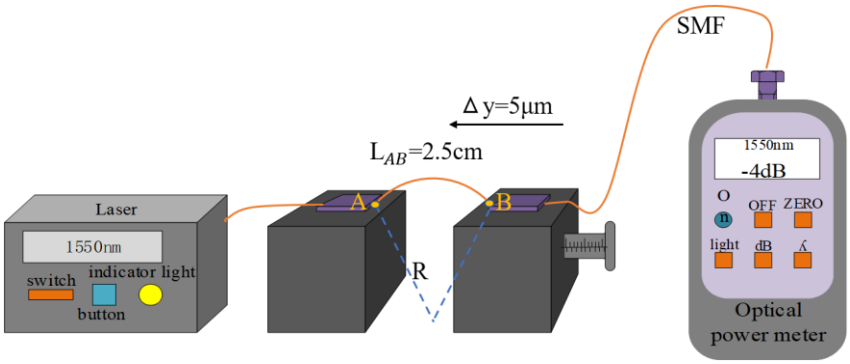

Fig. 2. Curvature measuring device.

Curvature is an important parameter in the practical application as well. The expression of curvature accuracy measurement is:

$$R=\frac{dC\times dP_{\min}}{dP} \tag{2}$$

where dP_{min}=10 nW is the minimum resolution unit of the optical power meter, and P is optical power. It has been calculated that the curvature accuracy 0.173 m^{-1}. The curvature response curves of five groups of side-polished fibers with different side-polished depths are shown in Fig. 3. The curvature sensing sensitivity of -10 dB is the best with -7.208 %/m^{-1}.

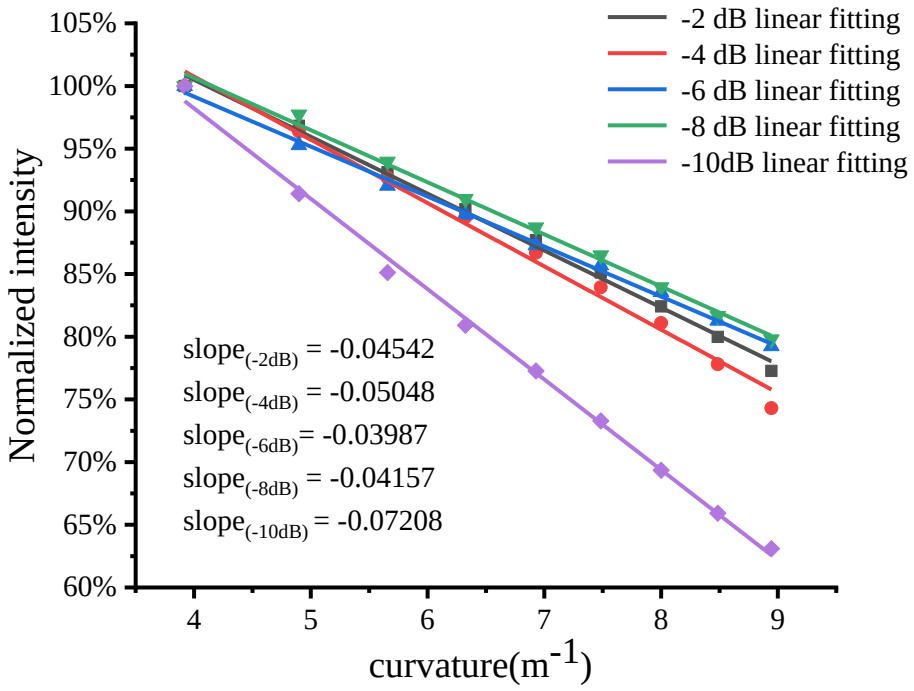

Fig. 3. -2 dB to -10 dB curvature and normalized light intensity linear fitting diagrams.

3. Design of monitoring system

In order to reduce the cost of the system and improve the integration and miniaturization of the system, LSFLD155 laser diode and LSIPD-A75 photodiode made from Beijing Light-sensing Technologies LTD were used as the laser source and photodetector. LSFLD155 laser diode has built-in monitoring photodiode (PD), high temperature resistance, low threshold and operating current. Photodiode LSIPD-A75 has the advantages of low dark current and high responsivity. Laser diode is a constant current driving element. In order to make the laser diode work statically for a long time, a 5 V-40 mA laser diode constant current driver module is adopted, as shown in Fig 4(e). The laser diode used in this paper produces a laser wavelength of

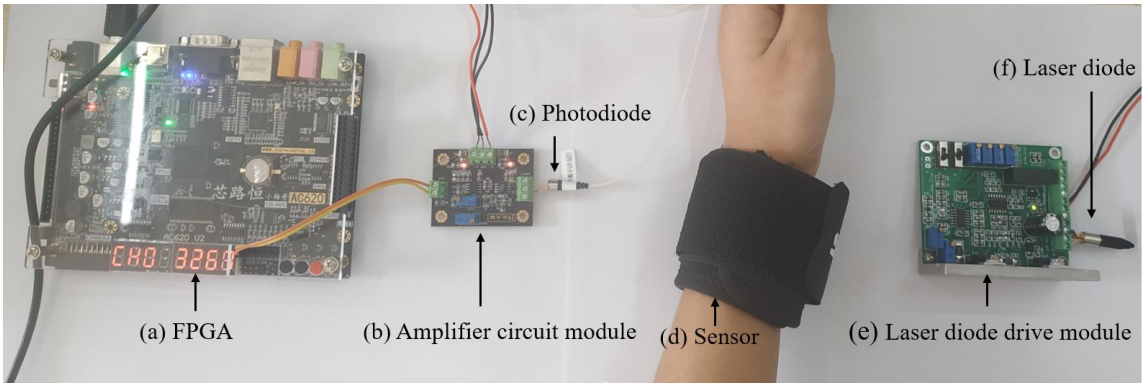

Fig. 4. Monitoring system diagram. (a) FPGA; (b) Current and voltage conversion and its amplifier circuit module; (c) Photodiode; (d) Sensor; (e) Laser diode drive module; (f) Laser diode.

1550 nm and a maximum output power of 4 mW. 9 V solar battery and step-down module are used to provide 5 V power for laser diode driver circuit, IV converter circuit and amplifier circuit. The IV

conversion circuit is based on the principle of transimpedance amplifier circuit [shown in Fig. 4(b)], and the optical signal is converted into electrical signal [45]. The IV conversion and amplification circuit have a maximum voltage amplification factor of 100. The FPGA development board manufactured by Wuhan Xinlu Heng Technology LTD was used to sample the signal. The whole monitoring system is shown in Fig 4. The D-shaped optical fiber curvature sensor is connected to laser diode at one end and IV conversion circuit at the other end. The IV conversion circuit is connected to FPGA, and FPGA is connected to PC for signal acquisition. The cost of the entire system does not exceed 100 dollars.

4. Pulse monitoring

A. Pulse Curvature Sensor Package

The exposed D-shaped single-mode fiber is fragile and needs to be protected in real applications. PDMS is used to encapsulate the exposed D-shaped single-mode fiber to enhance the strength of the sensor. As shown in Fig. 5(a), D-shaped optical fiber was fixed in the middle of the glass mold, with the D-shaped side up. The PDMS solution was prepared in accordance with 10:1, and then slowly dropped into the glass mold. After its surface was flat, it was slowly blown with a hot air gun to make it solidified. Finally, take out the D-shaped curvature sensor with a blade gently, which was shown in Figs. 5(b) and (c). Besides, in

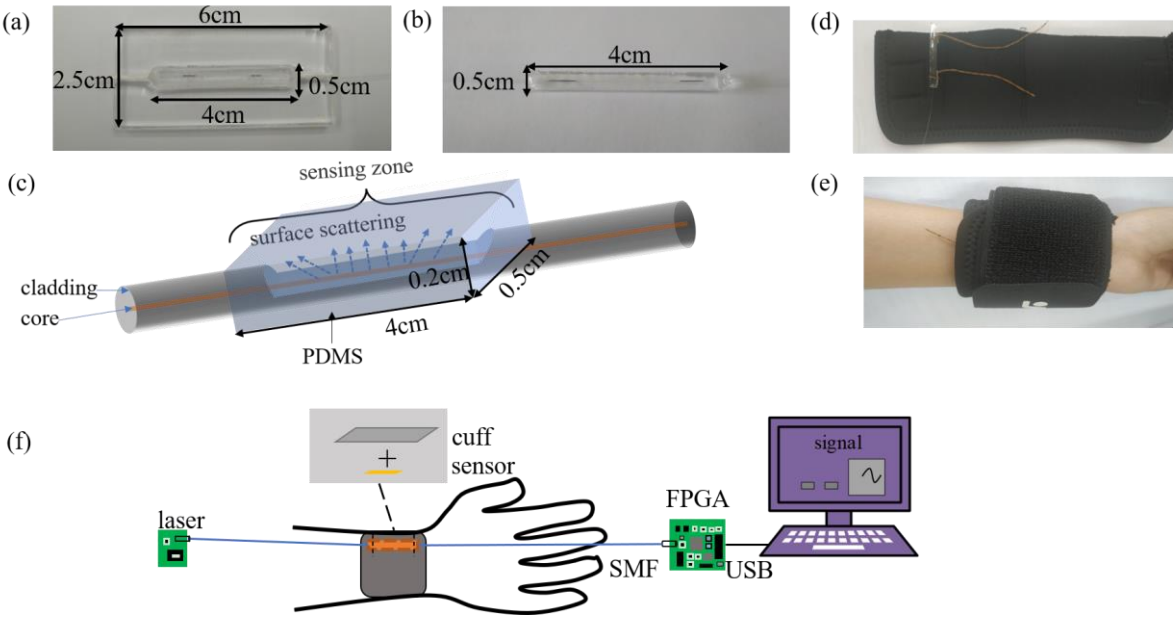

Fig. 5. (a) Glass mold; (b) Encapsulated D-shaped fiber optic curvature sensor; (c) Encapsulated D-shaped fiber curvature sensor model; (d) Both ends of the sensor are strapped to a wristband; (e) Wristbands with sensors are worn around the wrist; (f) Pulse monitoring system.

order to maintain the high sensitivity of encapsulated fiber, the sensor package size should not be too thick. The length of the encapsulated sensor is about 4 cm, the width and height are about 0.5 cm and 0.2 cm, respectively.

In order to make the sensor wearable and detachable, it is necessary to repackage the D-shaped sensor. As shown in Fig. 5(c), when the pulse signal needs to be collected, the two ends of the sensor are fixed on a soft cotton pad with two thin wires. One end of the thread is sewn onto the wristband and the other end is attached to two clips on the wristband. Then, the encapsulated sensor was wrapped on the pulse point of the wrist [shown in Fig. 5(d)]. The sensitive area rose or fell with the pulse, and the signal changed suddenly. Then, the wristband is attached to the wrist with Velcro, but the band should not be tied too tightly or it will reduce the sensitivity of the sensor, which made the pulse sensor sensitive and firm. What's more, when the breath signal needs to be collected, two thin wires on the sensor can be unwound and the sensor can be removed. A complete pulse monitoring system is shown in Fig. 5(e). The output voltage signal is collected by FPGA and transmitted to PC through serial port. The signal output by FPGA is sampled by the computer again. The sampling frequency of PC and FPGA are all adjusted to 500 Hz.

B. Static Pulse Signal Monitoring

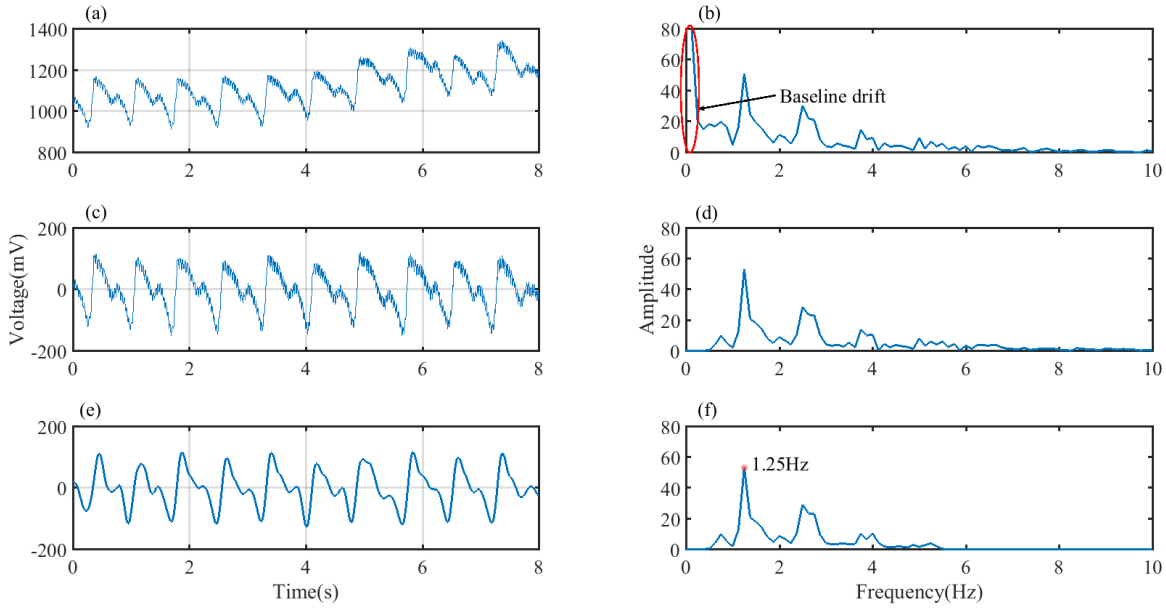

Fig. 6. Pulse signal pre-processing analysis: (a) Time-domain waveform of the original signal; (b) Frequency-domain of the original signal; (c) Time domain waveform of the signal after removing the baseline interference; (d) Frequency-domain of the signal after removing the baseline interference; (e) The time domain waveform of the signal after filtering out the high frequency noise; (f) Frequency domain waveform of the signal after filtering out high frequency noise.

The pulse data were preprocessed and analyzed, which was collected for 60s. In order to clearly and completely present the time domain characteristics of pulse in real time, the pulse signal of 8s were intercepted for processing and analysis at a time. The time domain waveform of initial pulse signal in 8s was shown Fig. 6(a). Through fast Fourier transform (FFT) of the initial pulse signal in 8s, the frequency domain spectrum of the original pulse signal was obtained, as shown in Fig. 6(b). There are baseline interference signals (low frequency noise) and high frequency noise in the original signal, which affect

signal analysis. In order to eliminate baseline drift and interference, pretreatment is required. Wavelet transform has the characteristics of time-frequency localization, multi-resolution and selection flexibility. Therefore, the wavelet filter can remove the noise and retain the signal mutation well, which is incomparable to the traditional method. The original signal wavelet is decomposed into 8 layers by db8 wavelet basis function. The low frequency approximation coefficient is set to zero to remove the baseline interference signal. The noise signal coefficient is set to zero to filter out high-frequency noise [44]. Fig 6(c) and (d) show the time-domain waveform and frequency-domain spectrum of the signal after removing the baseline interference. The time-domain waveform and frequency-domain spectrum after removing baseline interference and high-frequency noise are shown in Fig. 6(e) and (f). Above results demonstrated the proposed D-shaped fiber structure can be well applied to real-time monitoring of human pulse signal. Four volunteers were invited to collect pulse data. By comparing the time-frequency charts of 4 volunteers in Fig. 7(a)-(h), it can be concluded that their pulse frequencies in the stationary state are 1.25 Hz, 1.111 Hz, 1.085 Hz and 1.304 Hz, respectively. This is consistent with a healthy pulse rate in medical theory.

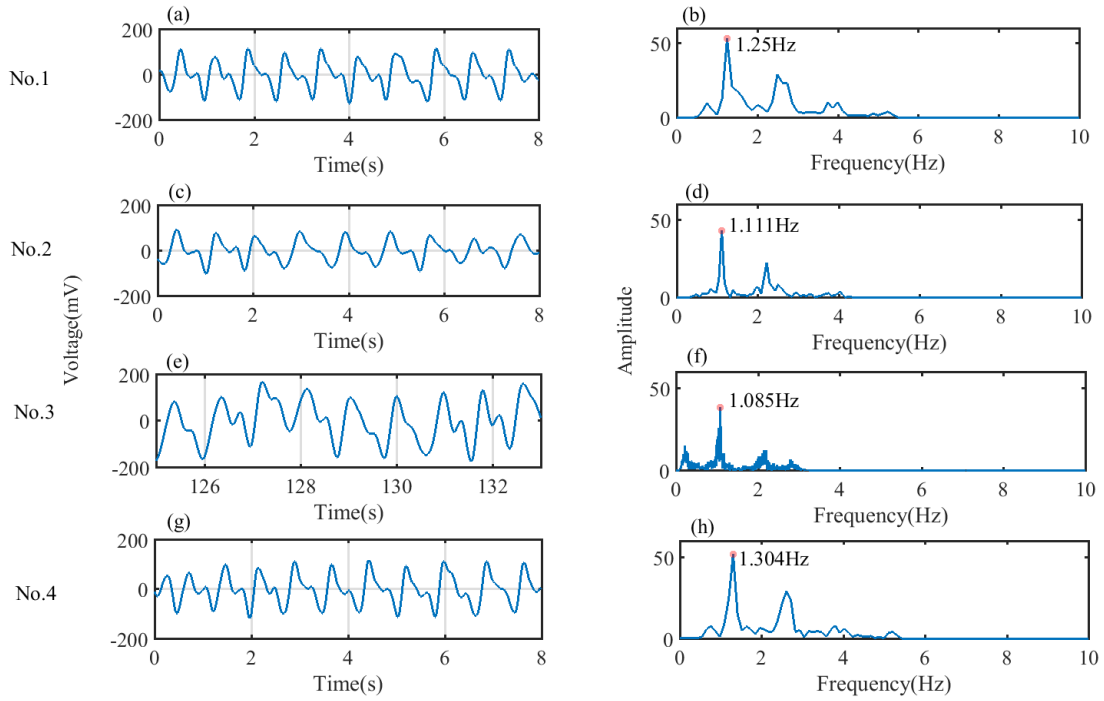

Fig. 7. Time-frequency graph of pulse rate data of 4 volunteers: (a), (c), (e) and (g): The time domain real-time acquisition signal after filtering and denoising; (b), (d), (f) and (h): Frequency domain spectrum diagram after filtering and denoising.

C. Pulse Signal Monitoring After Five Minutes of Jogging

Because the large vibration of the body and equipment during the exercise can affect the monitoring effect of the sensor and the frequency of human pulse is close to that of human stepping, this paper cannot carry out real-time monitoring of pulse during exercise. However, the pulse after jogging for 5min of volunteers No.1 ~ No. 4 in Fig. 7 were monitored, which was collected for 60s. And The pulse waveform in 10s in

time domain and frequency domain spectrum are shown in Fig. 8(a)-(d), respectively. The pulse intensity data, pulse frequency data and data changes before and after exercise of each volunteer are shown in Table I. By comparing pulse intensity and pulse frequency before and after exercise, it can be found that pulse intensity and frequency will be higher after exercise. After exercise, pulse intensity will be stronger than the original signal (without exercise), pulse frequency will increase to about 10 to 30 percent of higher than that of the original signal (without exercise). These results are consistent with the monitoring results of [46] and [47].

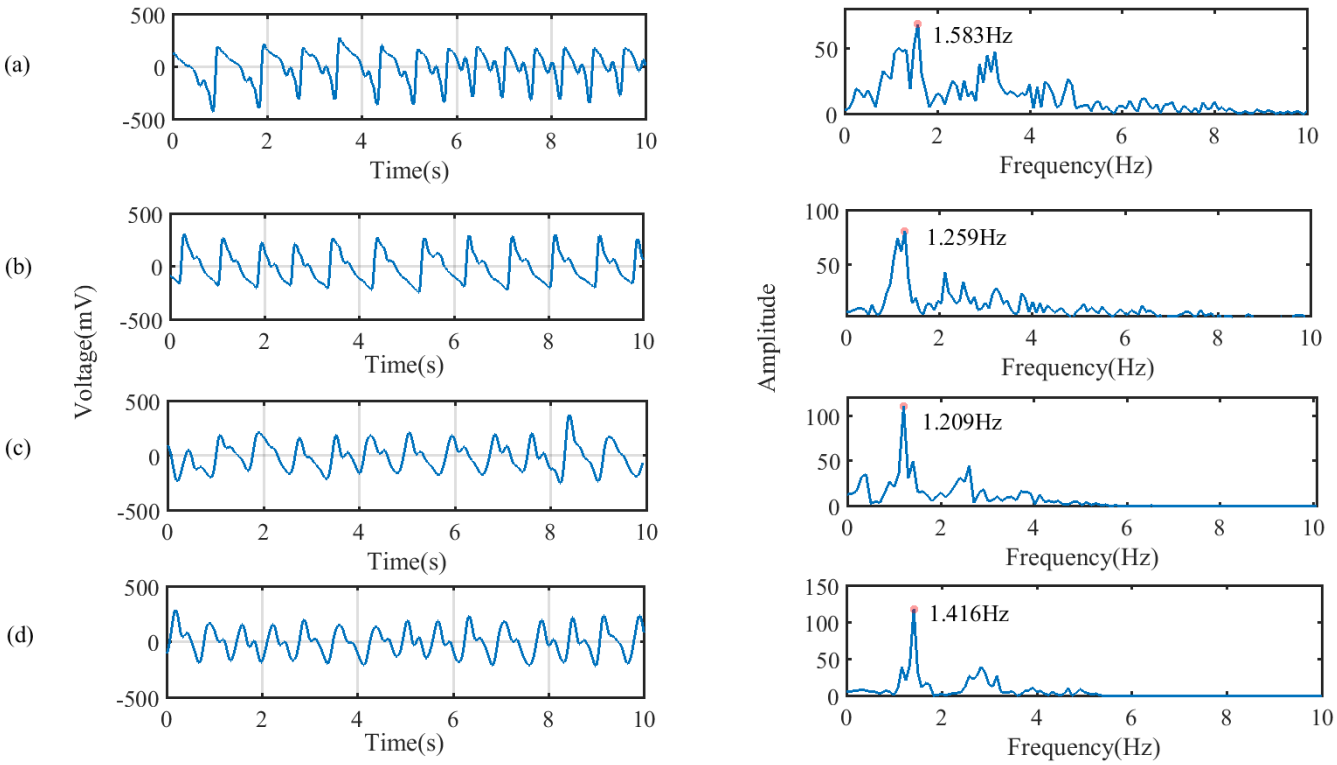

Fig. 8. Time domain pulse waveform and frequency domain spectrum of (a) No.1; (b) No.2; (c) No.3 and (d) No.4 volunteer after exercise.

TABLE I

Statistical table of pulse intensity change and pulse frequency change before and after 5-minute jogging

Volunteers	Pulse intensity before exercise (mv)	Pulse intensity after exercise (mv)	Pulse intensity changing value	Pulse rate before exercise (Hz)	Pulse rate after exercise (Hz)	Pulse rate changing value
No.1	216.2	521.6	241.3%	1.250	1.583	126.6%
No.2	146.7	465.7	317.5%	1.111	1.259	113.3%
No.3	242.4	382.5	157.8%	1.085	1.209	111.4%
No.4	201.8	388.1	192.3%	1.304	1.416	108.6%

5. Respiration monitoring

A. Respiratory signal acquisition

In addition, the D-shaped optical fiber curvature sensor is packaged into a wearable belt, which is applied to real-time monitoring of human respiratory signals. A rectangular silicone gasket is stitched under the D-shaped optical fiber structure encapsulated in PDMS [shown in Fig. 9(a)], which can effectively prevent the sensor from breaking in the process of respiratory monitoring. The length and width of the silicone gasket are 6 cm and 1 cm respectively, as shown in Fig. 9(b). Silicone spacers are attached to the elastic belt. When using, the elastic belt is tied to the place with the strongest respiratory intensity at the waist for signal collection, as shown in Fig. 9(c). The same as the pulse monitor, the sampling frequency of respiratory is adjusted to 500 Hz as well. The complete respiratory monitoring system is shown in Fig. 9(d).

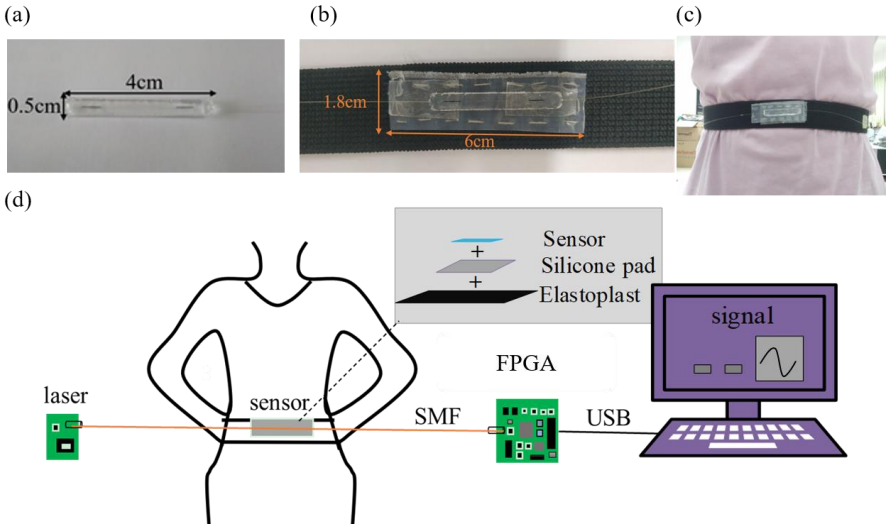

Fig. 9. (a) D-shaped fiber optic curvature sensor encapsulated with PDMS; (b) Sensors attached to belt; (c) Respiratory data collection volunteer; (d) Respiratory monitoring system.

B. Respiration Signal Preprocessing

The same as pulse signal processing, wavelet decomposition, reconstruction and noise removal techniques were used to remove baseline and noise from respiration data. According to the sampling frequency, respiration data were decomposed into 10 layers by db8 wavelet basis function. Fig. 10 shows the preprocessing results of respiratory signals in the quiet state and walking state respectively, which was collected for 120s and the respiratory signal of 60s were intercepted for processing and analysis at a time. Fig 10(a), (b), (g) and (h) show the time domain waveform and frequency domain spectrum of the original respiration signal in 60s. Fig 10(c), (d), (i) and (j) show the time domain waveform and frequency domain spectrum of the respiration signal in 60s after removing the baseline noise. Fig 10(e), (f), (k) and (l) show the final time domain waveform and frequency domain spectrum of the respiration signal in 60s after removing the baseline interference and high frequency noise. Experimental results indicate that the

respiratory signals of human body can be monitored in real time under the state of quiet and walking by the proposed D-shaped fiber optic curvature sensor.

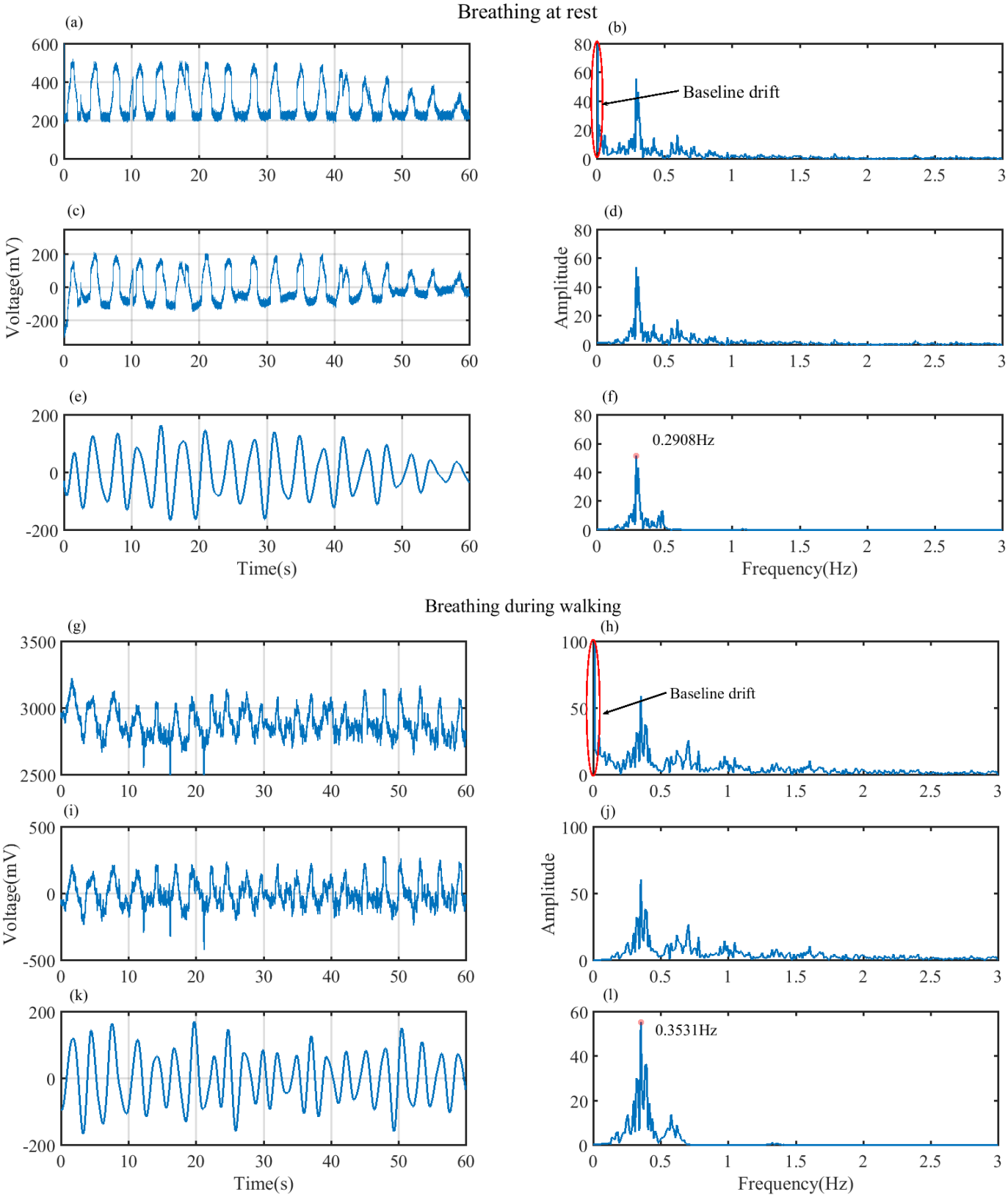

Fig.10. Respiration signal pre-processing analysis: (a), (g): Time-domain waveform of the original signal; (b), (h): Frequency-domain of the original signal; (c), (i): Time-domain waveform of the signal after removing the baseline interference; (d), (j):

Frequency-domain of the signal after removing the baseline interference; (e), (k): The time domain waveform of the signal after filtering out the high frequency noise; (f), (l): Frequency domain waveform of the signal after filtering out high frequency noise.

Finally, this paper compared the pulse and respiration monitoring system based on D-shaped curvature sensor with other systems with the same function. Parameters such as sensor types, sensor locations and manufacturing process complexity used in these systems are listed in Table II. Compared with these systems, the pulse respiration monitoring system based on D-shaped SMF curvature sensor proposed in this paper has a simpler manufacturing process and a lower cost and smaller size due to the low-cost light sources and photodetectors.

TABLE II

Comparison table

Sensor type	Monitoring object	Sensor location	Sensor fabrication	Size	Cost	Ref.
Diaphragm-based optical fiber	Pulse	Wrist	Complex	Small (1.5×1.5cm)	High	[48] (2019)
Capacitive	Pulse	Wrist	Simple	1.5×1.5cm	Low	[8] (2020)
Graphene-coated fiber	Pulse	Wrist	Less complex	0.8×1.3 cm	Low	[49] (2017)
Piezoelectric	Pulse	Neck & wrist	Complex	Small (length is 1 cm)	High	[50] (2017)
Optical fiber Michelson interferometer	Pulse	Wrist	Complex	Small (length is 1 cm)	High	[23] (2010)
SMS structure	Respiration	Abdomen(belt)	Simple	2.2×8 cm (light source) and 4×6 cm (PD)	High	[44] (2021)
D-shaped POF	Respiration	Abdomen(belt)	Simple	2.8×1.8 cm (light source) and 3.54×3.84 cm (optical receiver)	Low	[37] (2021)
Optical fiber MZI	Respiration	Mat	Complex	30×30 cm	High	[51] (2020)
Optical fiber FBG	Respiration	Nose (below)	Complex	-	High	[19] (2017)
D-shaped SMF	Pulse & respiration	Wrist (pulse), Abdomen (respiration)	Simple	Small (4×0.5×0.2cm)	Low	This work

6. Conclusion

A low-cost, wearable pulse and respiratory monitoring system based on D-shaped single-mode fiber curvature sensor has been proposed and experimentally studied. The curvature sensing performance is optimized and the best curvature sensitivity reach -7.208 %/m^{-1}. The laser source module and signal acquisition module in our system are integrated, miniaturized. In order to protect the fragile D-shaped single mode fiber and achieve good wearable comfort, the D-shaped fiber sensor is encapsulated by PDMS. The encapsulated sensor was fixed on the wrist band, and the pulse signals under different states were collected in real time by acquisition card based on FPGA. Fourier transform and wavelet analysis were used to remove baseline, denoise and time-frequency analysis. The results show that the curvature sensor can realize the real-time monitoring of pulse intensity and frequency, which has been proved by experiments before and after exercise, and agrees well to the health results of related medical theory. The D-shaped optical fiber curvature sensor is fixed on the elastic belt to realize the real-time monitoring of human respiration in the state of quietness and walking. The proposed system can provide an effective solution for personalized private health monitoring of the internet of things.

Acknowledgements

This work was jointly supported by National Natural Science Foundation of China (NSFC) (11864025, 62065013, 61865013 and 62175097); Natural Science Foundation of Jiangxi Province (Grant No. 20192ACB20031 and 20192ACBL21051), Key R&D Projects of the Ministry of Science and Technology of China (2018YFE0115700).

References

[1] Y. Li, M. J. Zhang, X. L. Hu, L. M. Yu, X. H. Fan, C. S. Huang, Y. L. Li, “Graphdiyne-based flexible respiration sensors for monitoring human health”, Nano Today, Vol. 39, pp. 101214, 2021.

[2] T. Dinh, T. Nguyen, H. P. Phan, N. T. Nguyen, D. V. Dao, J. Bell, “Stretchable respiration sensors: Advanced designs and multifunctional platforms for wearable physiological monitoring”, Biosensors and Bioelectronics, Vol. 166, pp. 112460, 2020.

[3] V. Sushmitha, K. Shivam, S. Rinky, B. Sushmee, “Direct growth of FeS2 on paper: A flexible, multifunctional platform for ultra-low cost, low power memristor and wearable non-contact breath sensor for activity detection”, Materials Science in Semiconductor Processing, Vol. 108, pp. 104910, 2020.

[4] Researchers at Kyung Hee University, “Willow-like portable triboelectric respiration sensor based on polyethylenimine-assisted CO2 capture”, Nanotechnology Weekly, Vol. 65, pp. 103990, 2019.

[5] T. Hiroyuki, Y. Masashi, T. Shunsuke, M. Takahiro, S. Yusuke, G. Takahisa, “Evaluation of respiratory rate monitoring using a microwave doppler sensor mounted on the ceiling of an intensive care unit: a prospective observational study”, Journal of Clinical Monitoring and Computing, pp. 1-9, 2021.

[6] T. Yudai, Y. Gu, N. Takaaki, A. Ryuzo, N. Toshiya, “Estimation of respiratory rate from thermography using respiratory

likelihood index", Sensors, 2021, Vol. 21, pp. 4406, 2021.

[7] F. Tomoko, T. Yuri, I. Hiroko, O. Makoto, N. Minoru, "Comparisons of the efficiency of respiratory rate monitoring devices and acoustic respiratory sound during endoscopic submucosal dissection", Journal of Clinical Monitoring and Computing, pp. 1-7, 2021.

[8] S. Sharma, A. Chhetry, M. Sharifuzzaman, et al, "Wearable capacitive pressure sensor based on MXene composite nanofibrous scaffolds for reliable human physiological signal acquisition", ACS Applied Materials & Interfaces, Vol. 12, no. 19, pp. 22212-22224, 2020.

[9] Y. Wu, P. Chen, Z. Hu, C. Chang, G. Lee and W. Yu, "A Mobile Health Monitoring System Using RFID Ring-Type Pulse Sensor," 2009 Eighth IEEE International Conference on Dependable, Autonomic and Secure Computing, pp. 317-322, 2009.

[10] Z. Kancleris, R. Simniskis, M. Dagys, V. Tamosiunas, "High power millimetre wave pulse sensor for W-band", IET Microwaves, Antennas & Propagation, Vol. 1, no. 3, pp. 113-123, 2007.

[11] T. Zhou, Y. X. Song, Y. P. Yuan, D. Q. Li, "A novel microfluidic resistive pulse sensor with multiple voltage input channels and a side sensing gate for particle and cell detection", Analytica Chimica Acta, Vol. 1052, pp. 113-123, 2019.

[12] Y. Xin, T. Liu, Y. Xu, J. F. Zhu, T. T. Lin, X. F. Zhou, "Development of respiratory monitoring and actions recognition based on a pressure sensor with multi-arch structures", Sensors and Actuators A: Physical, Vol. 296, pp. 357-366, 2019.

[13] E. D. Hurtado, A. Abusleme, J. A. P. Chávez, "Non-invasive continuous respiratory monitoring using temperature-based sensors", Journal of Clinical Monitoring and Computing, Vol. 34, pp. 223-231, 2020.

[14] A. Candiani, M. Konstantaki, A. Pamvouxoglou, & S. Pissadakis, "A shear sensing pad, based on ferrofluidic actuation in a microstructured optical fiber", IEEE Journal of Selected Topics in Quantum Electronics, Vol. 23, no. 2, pp. 210-216, 2016.

[15] G. T. Kanellos, G. Papaioannou, D. Tsiokos, C. Mitrogiannis, G. Nianios & N. Pleros, "Two dimensional polymer-embedded quasi-distributed FBG pressure sensor for biomedical applications", Optics Express, Vol. 18, no. 1, pp. 179-186, 2010.

[16] W. Bao, F. Chen, H. Lai, S. Liu & Y. Wang, "Wearable breath monitoring based on a flexible fiber-optic humidity sensor", Sensors and Actuators B: Chemical, Vol. 349, pp. 130794, 2021.

[17] L. S. Alwis, K. Bremer & B. Roth, "Fiber optic sensors embedded in textile-reinforced concrete for smart structural health monitoring: a review", Sensors, Vol. 21, no. 15, pp. 4948, 2021.

[18] H. L. Yu, S. Y. Wang, J. C. Wu, "Development of long-distance power supply system with high power laser over single mode fiber", Microwave and Optical Technology Letters, Vol. 63, no. 7, pp. 1995-1998, 2021.

[19] A. Manujlo, T. Osuch, "Temperature fiber bragg grating based sensor for respiration monitoring", The International Society for Optical Engineering, Vol. 10445, 2017.

[20] D. L. Presti, C. Massaroni, C. S. J. Leitão, et al, "Fiber Bragg gratings for medical applications and future challenges: A review", IEEE Access, Vol. 8, pp. 156863-156888, 2020.

[21] D. L. Presti, et al, "Cardio-respiratory monitoring in archery using a smart textile based on flexible fiber Bragg grating sensors", Sensors, Vol. 19, no. 16, pp. 3581, 2019.

[22] D. L. Presti, et al, "Wearable system based on flexible FBG for respiratory and cardiac monitoring", IEEE Sensors Journal, Vol. 19, no. 17, pp. 7391-7398, 2019.

[23] S. Eom, J. Park, J. Lee, "Optical fiber arterial pulse wave sensor", Microwave and Optical Technology Letters, Vol. 52, no. 6, pp. 1318-1321, 2010.

[24] N. Ushakov, A. Markvart, D. Kulik, L. Liokumovich, “Comparison of pulse wave signal monitoring techniques with different fiber-optic interferometric sensing elements”, Photonics, Vol. 8, no. 5, pp. 142, 2021.

[25] A. Miliou, “In-Fiber Interferometric-Based Sensors: Overview and Recent Advances”, Photonics, Multidisciplinary Digital Publishing Institute, Vol. 8, no. 7, pp. 265, 2021.

[26] Y. H. Hsieh, N. K. Chen, “Micro tapered Mach-Zehnder fiber interferometer for monitoring pressure fluctuation and its applications in pulse rate detection”, 2013 6th IEEE/International Conference on Advanced Infocomm Technology (ICAIT), pp. 113-115, 2013

[27] F. Tan, S. Chen, W. Lyu, Z. Y. Liu, C. Y. Yu, C. Lu, H. Y. Tam, “Non-invasive human vital signs monitoring based on twin-core optical fiber sensors”, Biomedical Optics Express, Vol. 10, no. 11, pp. 5940-5952, 2019.

[28] V. Zenzen, H. Zankl, “Protoporphyrin IX-accumulation in human tumor cells following topical ALA-and h-ALA-application in vivo”, Cancer Letters, Vol. 202, pp. 35-42, 2003.

[29] S. Demetrio, S. Salvador, “Low-cost plastic optical fiber pressure sensor embedded in mattress for vital signal monitoring”, Sensors (Basel, Switzerland), Vol. 17, no. 12, pp. 2900, 2017.

[30] G. Yin, F. Zhang, B. Xu, J. He & Y. Wang, “Intensity-modulated bend sensor by using a twin core fiber: theoretical and experimental studies”, Optics Express, Vol. 28, no. 10, pp. 14850-14858, 2020.

[31] X. Yang, Z. Chen, C. S. M. Elvin, L. H. Y. Janice, S. H. Ng, J. T. Teo & R. Wu, “Textile fiber optic microbend sensor used for heartbeat and respiration monitoring”, IEEE Sensors Journal, Vol. 15, no. 2, pp. 757-761, 2014.

[32] Y. Xiao, C. Shen, S. Shuai, J. Gong, Z. Liu and Z. Sun, “Fiber optic sensor based on MZI to measure urine sugar and micro velocity simultaneously,” 2018 Asia Communications and Photonics Conference (ACP), 2018.

[33] A. Aitkulov, and D. Tosi, “Optical fiber sensor based on plastic optical fiber and smartphone for measurement of the breathing rate”, IEEE Sensors Journal, Vol. 19, no. 9, pp. 3282-3287, 2019.

[34] Y. Li, B. Dong, E. Chen, X. Wang, Y. Zhao, W. Zhao, Y. Wang, “Breathing process monitoring with a biaxially oriented polypropylene film based fiber fabry-perot sensor”, Optics Communications, Vol. 475, pp. 126292, 2020.

[35] M. Życzkowski, M. Szustakowski, W. Ciurapiński, B. Uziębło-Życzkowska, “Interferometric fiber optics based sensor for monitoring of the heart activity”, Acta Phys. Pol. A, Vol. 120, no. 4, pp. 782-784, 2021.

[36] N. V. Kumar, S. Pant, S. Sridhar, V. Marulasiddappa, S. Asokan, “Fiber bragg grating based pulse monitoring device for real-time non-invasive blood pressure measurement-a feasibility study”, IEEE Sensors Journal, Vol. 21, no. 7, pp. 9179-9185, 2021.

[37] Y. L. Wang, B. Liu, Y. N. Pang, J. Liu, J. L. Shi, S. P. Wan, X. D. He, J. H. Yuan, Q. Wu, “Low-cost wearable sensor based on a D-shaped plastic optical fiber for respiration monitoring”, IEEE Transactions on Instrumentation and Measurement, Vol. 70, pp. 1-8, 2021.

[38] Y. Zheng, et al. “Design, sensing principle and testing of a novel fiber optic displacement sensor based on linear macro-bending loss”, Optik-International Journal for Light and Electron Optics, Vol. 242, pp. 167194, 2012.

[39] H. Kumar, U. Ramani, B. K. Singh, et al. “Investigations on the highly sensitive metal-coated broad range D-shaped optical fiber refractive index sensor”, Plasmonics, pp. 1-9, 2021.

[40] Y. Ying, J. K. Wang, K. Xu, G. Y. Si, “High sensitivity D-shaped optical fiber strain sensor based on surface plasmon resonance”, Optics Communications, Vol. 460, pp. 125147, 2020.

[41] N. A. A. Kadir, N. Irawati, A. A. A. Jafry, N. M. Razali, A. Hamzah, S. W. Harun, “Sodium nitrate sensor based on D-shaped fiber structure”, Measurement, Vol. 163, pp. 107927, 2020.

[42] S. Wang, X. H. Sun, Y. H. Luo, G. D. Peng, “Surface plasmon resonance sensor based on D-shaped Hi-Bi photonic crystal

fiber", Optics Communications, Vol. 467, pp.125675, 2020.

[43] S. M. Chandani, "Fibre optic sensors based on D-shaped elliptical core fibres", University of British Columbia, 2007.

[44] Y. N. Pang, B. Liu, J. Liu, S. P. Wan, T. Wu, X. D. He, J. Yuan, X. Zhou, K. Long, and Q. Wu, "Wearable optical fiber sensor based on a bend single mode-multimode-single mode fiber structure for respiration monitoring", IEEE Sensors Journal, Vol. 21, no. 4, pp. 4610-4617, 2021.

[45] H. Q. Tay. "An improvement of the current–voltage conversion technique in over-current sensing circuit for low-power low dropout linear voltage regulators", Analog Integrated Circuits and Signal Processing, Vol. 85, no. 2, pp. 237-242, 2015.

[46] J. He, P. Xiao, W. Lu, J. W. Shi, L. Zhang, Y. Liang, C. F. Pan, S. W. Kuo, T. Chen, "A Universal high accuracy wearable pulse monitoring system via high sensitivity and large linearity graphene pressure sensor", Nano Energy, Vol. 59, pp. 422-433, 2019.

[47] T. D. Chen, G. C. Yang, J. Q. Wang, L. M. Ma, S. R. Yang, "Surfactant stabilized go liquid crystal for constructing double-walled honeycomb-like go aerogel with super-sensitivity for fingertip pulse monitoring", Carbon, Vol. 184, pp. 53-63, 2021.

[48] J. Wang, K. Liu, Q. Sun, et al, "Diaphragm-based optical fiber sensor for pulse wave monitoring and cardiovascular diseases diagnosis", Journal of Biophotonics, Vol. 12, no. 10, 2019.

[49] S. Zang, Q. Wang, Q. Mi, J. Zhang, & X. Ren, "A facile, precise radial artery pulse sensor based on stretchable graphene-coated fiber", Sensors and Actuators A: Physical, Vol. 267, pp. 532-537, 2017.

[50] D. Y. Park, D. J. Joe, D. H. Kim, et al, "Self-powered real-time arterial pulse monitoring using ultrathin epidermal piezoelectric sensors", Advanced Materials, Vol. 29, no. 37, 2017.

[51] S. Wang, X. L. Ni, L. Y. Li, J. Y. Wang, Q. Liu, Z. J. Yan, L. Zhang, and Q. Z. Sun, "Noninvasive monitoring of vital signs based on highly sensitive fiber optic mattress," IEEE Sensors Journal, Vol. 20, no. 11, pp. 6182-6190, 2020.